

Powered Swing-By in the Elliptic Restricted Problem

Alessandra F. S. Ferreira¹ and Antonio F. B. A. Prado²

Instituto Nacional de Pesquisas Espaciais, São José dos Campos, São Paulo, 12227-010, Brazil

Othon C. Winter³

Universidade Estadual Paulista, Guaratinguetá, São Paulo, 12516-410, Brazil

This paper studies maneuvers for a spacecraft that combines an impulse with a Swing-By performed with a celestial body that is traveling in an elliptical orbit around the primary body of the system. The objective is to measure the variations of the velocity, energy and angular momentum of the spacecraft due to this maneuver. An algorithm is developed to obtain the energy and the angular momentum variation for this particular type of powered Swing-By. In this way, it is possible to find the best direction and instant to apply the impulse in order to maximize the energy variation. The results show that applying the impulse in the direction of the motion of the spacecraft is generally not the optimal solution and the results depends on the position of the secondary body in its orbit around the main body and the eccentricity of the orbits of the primaries. Compared to the circular case, several situations where the impulse is retrograde appears when the secondary body is at the periapsis of its orbit, due to the larger gains that can be obtained from the new geometry of the Swing-By.

Nomenclature

α	=	angle that defines the impulse direction
ΔE	=	variation of energy
ΔE_{\max}	=	maximum variation of energy
δV	=	magnitude of the impulse
$\delta \mathbf{V}$	=	impulse vector
e	=	eccentricity of the orbits of M_1 and M_2
f	=	generic function
M_1	=	primary body
M_2	=	secondary body
M_3	=	spacecraft with negligible mass
μ	=	mass of the secondary body
m_1	=	actual mass of M_1
m_2	=	actual mass of M_2
v	=	true anomaly of M_2 relative M_1
P	=	periapsis of the orbit
ψ	=	approach angle
Q	=	point of application of the impulse
r	=	magnitude of the position vector
\mathbf{r}	=	position vector
r_p	=	magnitude of the radius of the periapsis
\mathbf{r}_p	=	periapsis vector radius

¹ Doctoral student, Division of Space Dynamics and Control, INPE, Av dos Astronautas 1758, São José dos Campos, São Paulo, 12227-010, Brazil.

² Head of Division, Division of Space Dynamics and Control, INPE, Av dos Astronautas 1758, São José dos Campos, São Paulo, 12227-010, Brazil. AIAA Associate Fellow.

³ Professor, Department of Mathematics, Universidade Estadual Paulista, Guaratinguetá, São Paulo, 12516-410, Brazil.

θ	=	true anomaly of M_3 relative to M_2
V_{p^-}	=	velocity of the spacecraft in the first orbit at the point where the impulse is applied
V_{p^+}	=	velocity of the spacecraft in the second orbit at the point where the impulse is applied
V_{inf^-}	=	magnitude of the velocity when the spacecraft approaches M_2
V_{inf^+}	=	magnitude of the velocity when the spacecraft leaves M_2
V_2	=	linear velocity of M_2 with respect to M_1
V_p	=	magnitude of the velocity of the spacecraft at the periapsis

I. Introduction

THE powered Swing-By occurs when a satellite makes a close approach maneuver with a celestial body and uses the gravity of this body, combined with the application of an impulse, to gain or lose energy. The usual objective of this type of maneuver is the fuel economy on space missions, but other possibilities also exist, like adjusting the timing of a more complex maneuver.

The dynamics used in the present research is the elliptical restricted three body problem, which means that the system is assumed to be formed by two massive bodies, called M_1 and M_2 , in elliptical orbits around their center of mass and a third body M_3 , with negligible mass, which has its motion restricted to the orbital plane of the primaries.

The objective is to measure the behavior of the energy of the spacecraft as a function of the three parameters of the standard Swing-By: V_{inf^-} , the velocity of approach of the spacecraft; r_p , the periapsis distance of the orbit of the spacecraft around the secondary body; and ψ , the angle of approach, which specifies the geometry of the approximation; the two parameters that defines the format of the orbit of the primaries: the eccentricity of the orbits (e) and the true anomaly (v) of the secondary body at the moment of the close encounter with the spacecraft; and the three parameters that specify the impulse applied (δV , the magnitude of the impulse; θ , the position that specifies the point of application of the impulse; and α , the direction of the application of the impulse in the orbit of the spacecraft around the secondary body). Our study makes a mapping of those orbits, identifying the ones that can be more interesting for space missions.

Starting from given initial conditions, the algorithm makes numerical integrations of the equations of motion forward in time (with the application of the impulse) from the periapsis until the spacecraft reaches a region far from the secondary body, to get the information about the energy and angular momentum after the close approach. After that the numerical integration is performed backwards in time, again starting at the periapsis, but now without the impulse, to get the values of the energy and angular momentum before the powered swing-by. The integrations in both senses of time are made until the spacecraft reaches a distance from M_2 that is half of the distance M_1 - M_2 , to ensure that the distance between the spacecraft and M_2 is large enough such that the effects of this secondary body can be neglected.

Applications of this type of research are general and can be applied to any system of primaries that has an eccentricity. A very good example in the Solar System in the dwarf planet Haumea, which has one of its moons with eccentricity in the order of 0.25. A mission to this planet may use a propelled Swing-By, like the one proposed here, in that moon, to help the capture of the spacecraft by the system or in maneuvers during the mission, to make the spacecraft to go from one body to the other of this triple system. Other potential applications are in one of the many systems with larger eccentricities that are being discovered outside the Solar System lately. In all those cases the eccentricity of the orbits must be taken into consideration, since its effects are strong. This research is a continuation of two previous publications: Prado¹, which studied the effect of the propelled Swing-By, but restricted to the case of circular orbits; and Prado², who studied Swing-By maneuvers using the elliptic restricted three-body problem, but without the application of an impulse. Another application would be, for example, in the Aster mission, a project that consists of sending a spacecraft to a triple asteroid^{3,4}. Regarding the elliptical restricted three-body problem, in the literature, it is also available the work by Broucke⁵, where a systematic study is made to verify the main differences in the stability properties of periodic orbits in the circular and elliptical problems.

II. Powered Swing-By

The Powered Swing-By is the maneuver that combines the standard Swing-By^{6,7,8}, where the spacecraft makes an unpowered close approach with a celestial body, with the application of an impulse to the spacecraft during this passage. The impulse can have any magnitude and any direction in space. The literature has many papers related to the Swing-By maneuver, like in McConaghy, Debban, Petropoulos, Longuski⁹ and Okutsu, Yam, Longuski¹⁰, which presents Swing-By maneuvers combined with low thrust.

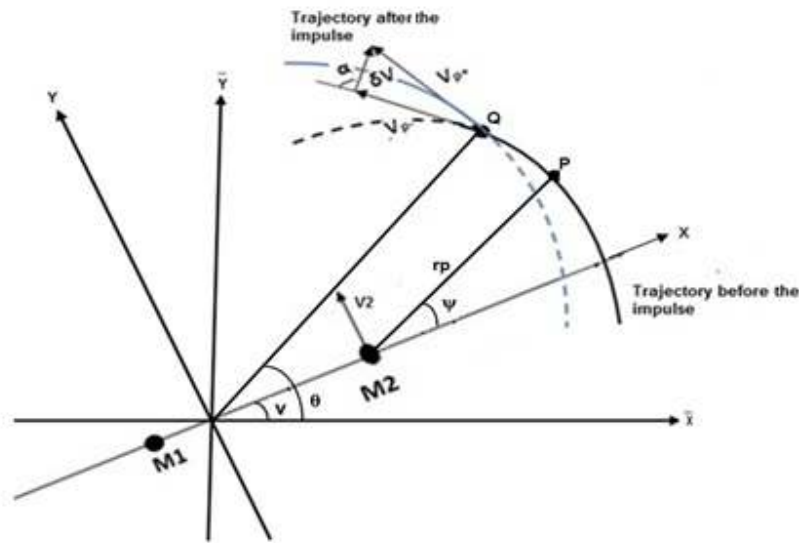


Figure 1. Geometry of the Powered Swing-By.

Figure 1 shows the geometry of the maneuver studied here. The variables shown are: M_1 and M_2 , the primary and the secondary body of the system, respectively; V_2 , the velocity vector of M_2 around the center of mass of the system M_1 - M_2 ; ψ , the angle of approach; P , the periapsis, which is the point of the shortest distance between M_2 and M_3 ; r_p , the vector radius of the periapsis; V_{p-} , the velocity vector of the spacecraft at the periapsis of the first orbit before the impulse is applied; V_{p+} , the same velocity vector of the spacecraft, but now after the impulse is applied; δV , vector that represents the impulse applied; α , the angle between V_p and δV , which defines the direction of the impulse (clockwise is positive); θ , the angle that defines the point where the impulse is applied (counterclockwise is positive). The step-by-step powered Swing-By maneuver algorithm is now described:

- We started the study with the spacecraft placed at the point P . This was done by specifying values for the three variables that uniquely define a Swing-By trajectory: V_p , r_p , and ψ ;
- From the point P , it was performed a numerical integration in reverse time¹¹, until the spacecraft reaches half of the distance M_1 - M_2 . At this point the energy, velocity and angular momentum before the maneuver are calculated;
- After that it is applied the impulse δV at the point P , forming an angle α with the direction of the motion of the spacecraft. The magnitude and direction of the impulse were varied to search for the values that maximize the energy variation;
- After the application of this impulse, the orbit was integrated forward in time, again until a point distant from M_2 is reached (defined as half of the M_1 - M_2 distance, as done before), so giving the values for the energy, velocity and angular momentum after the maneuver is completed;
- Finally, the variations of energy, as a function of the magnitude of the impulse, the angle that defines the position of the point where the impulse is applied and the angle that defines the direction of the impulse, were calculated. This magnitude can be written as:

$$\Delta E = f(\delta V, \theta, \alpha) \quad (1)$$

III. Elliptic Restricted Three Body Problem

The maneuvers shown here are studied using the elliptic restricted three body problem. The system is assumed to be formed by two massive bodies, M_1 called primary, and M_2 called secondary, in elliptical trajectories around their center of mass and a third body M_3 , with negligible mass and which motion is restricted to the orbital plane of the primaries.

The canonical system of units is used, so the unit of distances become the semi-major axis of the orbit of M_1 and M_2 , the mass of the secondary body (M_2) is $\mu = \frac{m_2}{(m_1 + m_2)}$, the mass of the primary M_1 is $1-\mu$, m_1 and m_2 being the actual masses of the bodies M_1 and M_2 , respectively. The time unit is chosen such that the period of the motion of the two primaries is 2π . In this system the gravitational constant becomes one.

There are several systems of reference that can be used to study this problem¹². The most used ones are the fixed and the rotating systems. The fixed reference system (inertial) was used for the numerical integrations. In this system the origin is located in the center of mass of the primaries and the horizontal axis is the line connecting both primaries at the beginning of the study. In the rotating system the horizontal axis follows the motion of the two primaries. Figure 2 shows both systems.

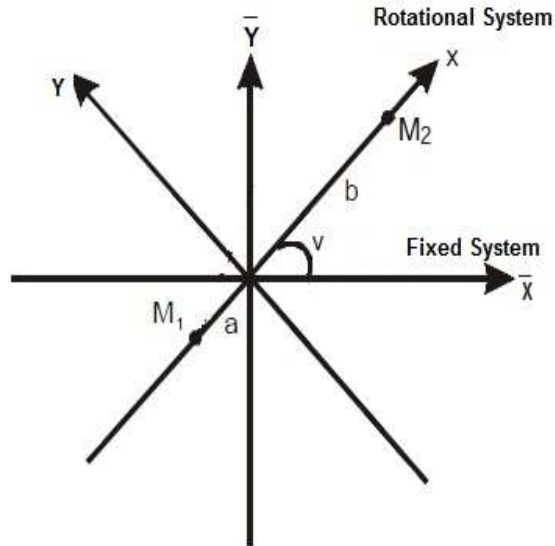


Figure 2. Fixed and rotational reference systems.

Since in the fixed system both primaries follow elliptical orbits, the equations for \bar{x}_1 , \bar{y}_1 and \bar{x}_2 , \bar{y}_2 are given by (the angle v is the true anomaly of M_2):

$$\bar{x}_1 = -\mu r \cos v \quad (2)$$

$$\bar{y}_1 = -\mu r \sin v \quad (3)$$

$$\bar{x}_2 = (1 - \mu) r \cos v \quad (4)$$

$$\bar{y}_2 = (1 - \mu) r \sin v \quad (5)$$

The equations of motion for the elliptic restricted three body problem are given by:

$$\ddot{\bar{x}} = -\frac{(1 - \mu)(\bar{x} - \bar{x}_1)}{r_1^3} - \frac{\mu(\bar{x} - \bar{x}_2)}{r_2^3} \quad (6)$$

$$\ddot{\bar{y}} = -\frac{(1 - \mu)(\bar{y} - \bar{y}_1)}{r_1^3} - \frac{\mu(\bar{y} - \bar{y}_2)}{r_2^3} \quad (7)$$

The two dots over \bar{x} and \bar{y} represent the second derivative with respect to time, r_1 is the distance between M_1 and M_3 and r_2 is the distance between M_2 and M_3 . They are given by:

$$r_1^2 = (\bar{x} - \bar{x}_1)^2 + (\bar{y} - \bar{y}_1)^2 \quad (8)$$

$$r_2^2 = (\bar{x} - \bar{x}_2)^2 + (\bar{y} - \bar{y}_2)^2 \quad (9)$$

IV. Results

The goal of the present paper is to understand the effects that the eccentricity of the primaries and the position of M_2 relative to the position of M_1 cause in the trajectory of a spacecraft that makes a powered Swing-By with the secondary body.

We considered cases with $\psi = 270^\circ$ (the geometry that gives the largest increase of energy) and eccentricity zero (to serve as a comparison), 0.1, 0.2, 0.3, 0.4 and 0.5. For each value of the eccentricity (except $e = 0$) orbits where the true anomaly of M_2 at the moment of the close approach equals to 0° , 90° , 180° and 270° were used. The impulse ranged from 1.0 to 4.0 canonical units, with α and θ varying from -180° to 180° , both of them with a step of 1.0 degree. For the first set of simulations, which considered a generalized Earth-Moon system, that is a system that has the same mass parameter of the Earth and the Moon, but has different values for the eccentricity we used $r_p = 0.00495$ canonical units and $\mu = 0.01214$, that is the mass parameter of the Earth-Moon system.

Figures 3 and 4 show the results for the cases with $e = 0.0$ and Figs. 5 and 6 show the results for $e = 0.2$, both cases using a magnitude for the impulse of 1.0 and 2.0 canonical units. Other cases have been studied, but are not shown here due to the similarities of the results. In the graphs, the contour lines represents the variation of the energy (in canonical units) as a function of α and θ . The horizontal axis represents the angle that defines the direction of the impulse (α) and the vertical axis shows the angle that defines where the impulse is applied, θ , which is the angle that the point where the impulse is applied, measured in the inertial system of reference, makes with the periaapsis of the incoming orbit. It is defined such that it is positive in the counterclockwise direction.

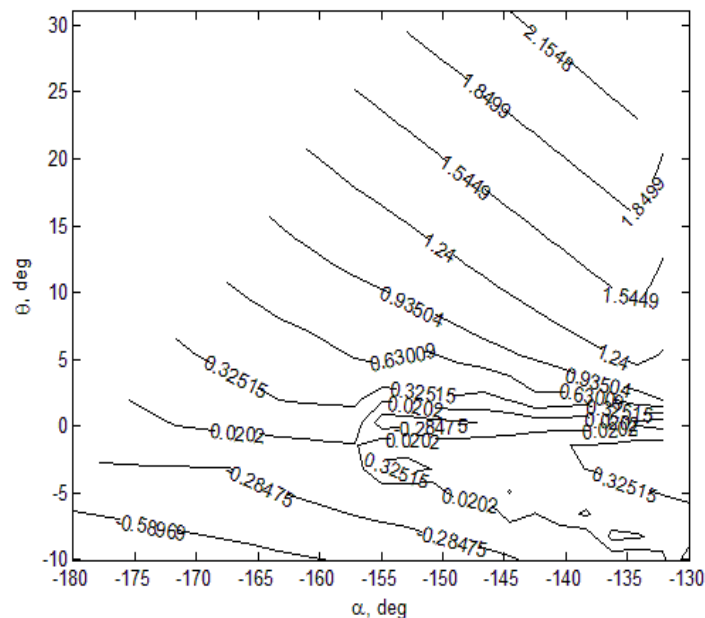


Figure 3. Variation of energy (in canonical units) as a function α and θ , for $e = 0$ and $\delta V = 1.0$ C.U.

When $e = 0$ and $\delta V = 1.0$ C.U., the maximum variation of energy is 2.49337 canonical units. In the graph this value is at the top right side. The empty regions of the curves represent trajectories ending in captures or collisions. The value of α in the region shown indicates a retrograde impulse, which reduces the velocity of the spacecraft in order to make a large curvature in the trajectory of the spacecraft around the secondary body, so gaining more energy from the gravitational part of the maneuver, which compensates the loss of energy due to the retrograde impulse. For $e = 0$ and $\delta V = 2.0$ C.U., it is possible to note that the maximum variation of energy increases significantly. It is 8.34465 canonical units and it is located in the point where $\alpha = -19^\circ$ and $\theta = 1.000491^\circ$. This fact happens because the magnitude of the impulse is twice the previous one and this fact influences the results. The impulse is no longer retrograde, because with this higher magnitude the impulse has an important component in the maneuver and now, instead of retrograde, the impulse only deviates the spacecraft in the direction of the secondary body, to increase the gains of the gravitational part of the maneuver, but still using a direction that increases the energy of the spacecraft due to the impulse itself. The same occurs for values of the magnitude of the impulse greater than 2.0 C.U.

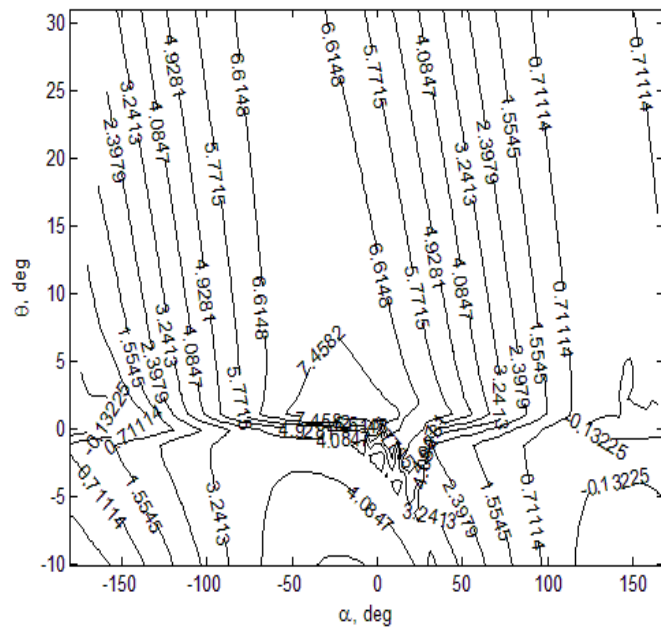


Figure 4. Variation of energy (in canonical units) as a function α and θ , for $e = 0$ and $\delta V = 2.0$ C.U.

Figure 5 presents the variation of energy for the cases $e = 0.2$, $\delta V = 1.0$ C.U., $v = 0^\circ, 90^\circ, 180^\circ$ and 270° , being v the true anomaly of the secondary body at the moment of the close encounter with the spacecraft.

Once again, the empty regions represent conditions that resulted in captures or collisions. Figure 6 presents the variation of energy for the cases $e = 0.2$, $\delta V = 2.0$ C.U., $v = 0^\circ, 90^\circ, 180^\circ$ and 270° . The empty regions are again trajectories that resulted in captures or collisions.

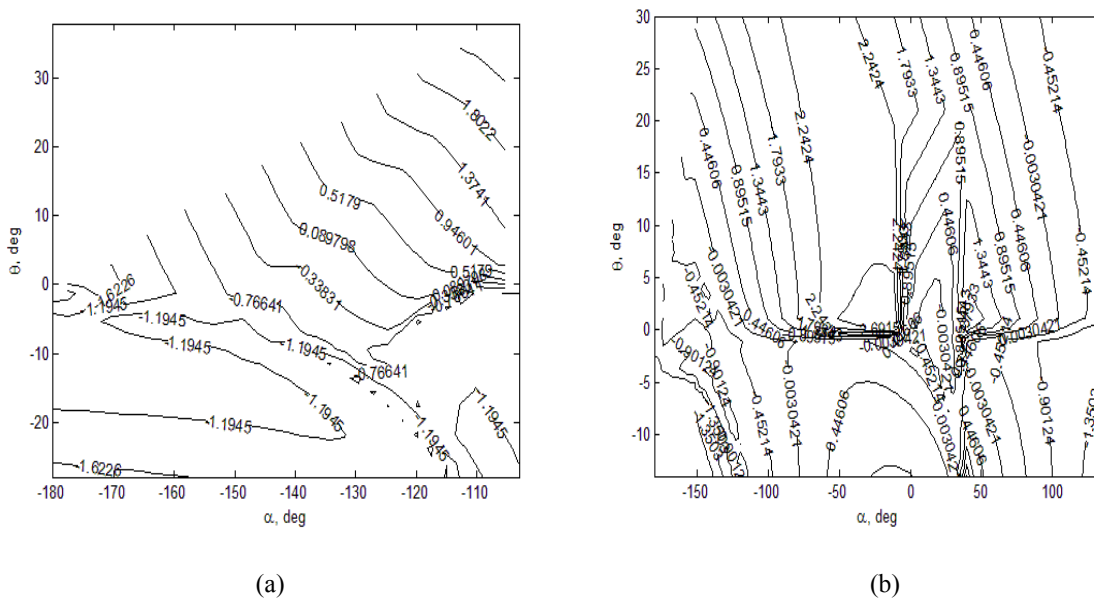


Figure 5. Variation of energy (in canonical units) as a function α and θ , for $e = 0.2$, $\delta V = 1.0$ C.U., (a) $v = 0^\circ$, (b) $v = 90^\circ$, (c) $v = 180^\circ$ and (d) $v = 270^\circ$.

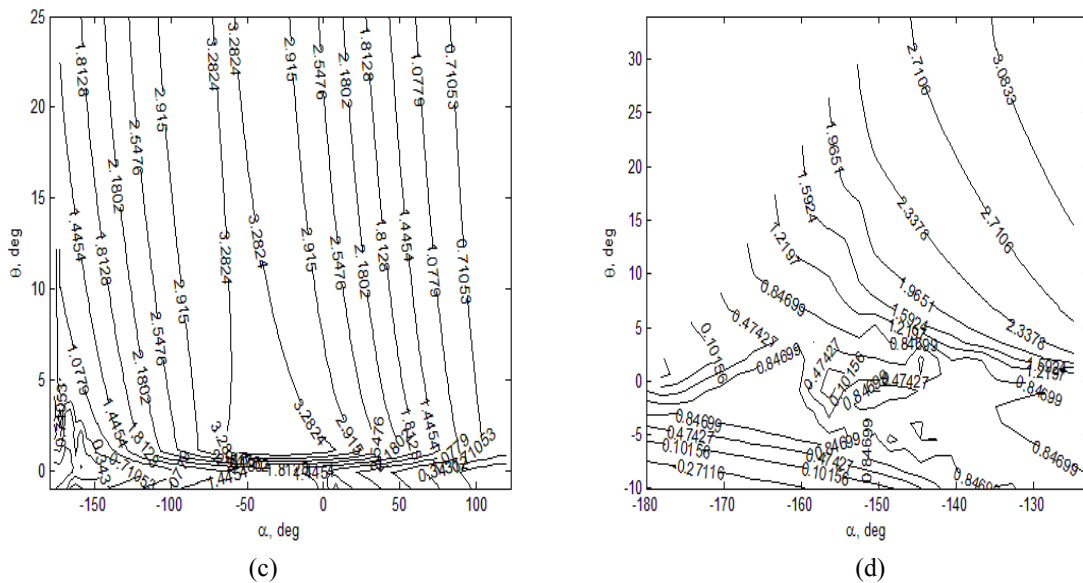


Figure 5 (cont). Variation of energy (in canonical units) as a function α and θ , for $e = 0.2$, $\delta V = 1.0$ C.U., (a) $\nu = 0^\circ$, (b) $\nu = 90^\circ$, (c) $\nu = 180^\circ$ and (d) $\nu = 270^\circ$.

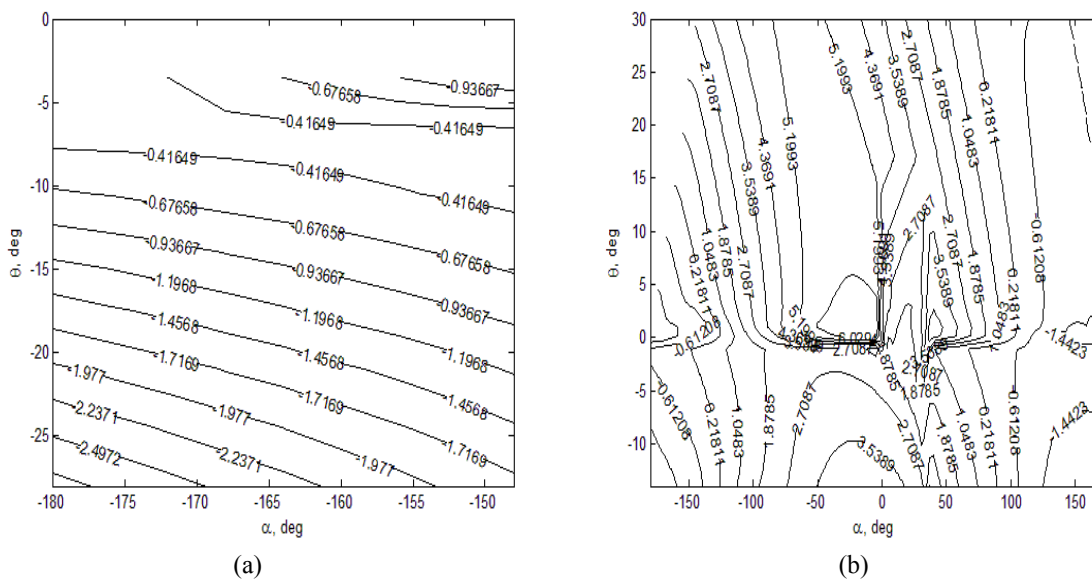


Figure 6. Variation of energy (in canonical units) as a function α and θ , for $e = 0.2$, $\delta V = 2.0$ C.U., (a) $\nu = 0^\circ$, (b) $\nu = 90^\circ$, (c) $\nu = 180^\circ$ and (d) $\nu = 270^\circ$.

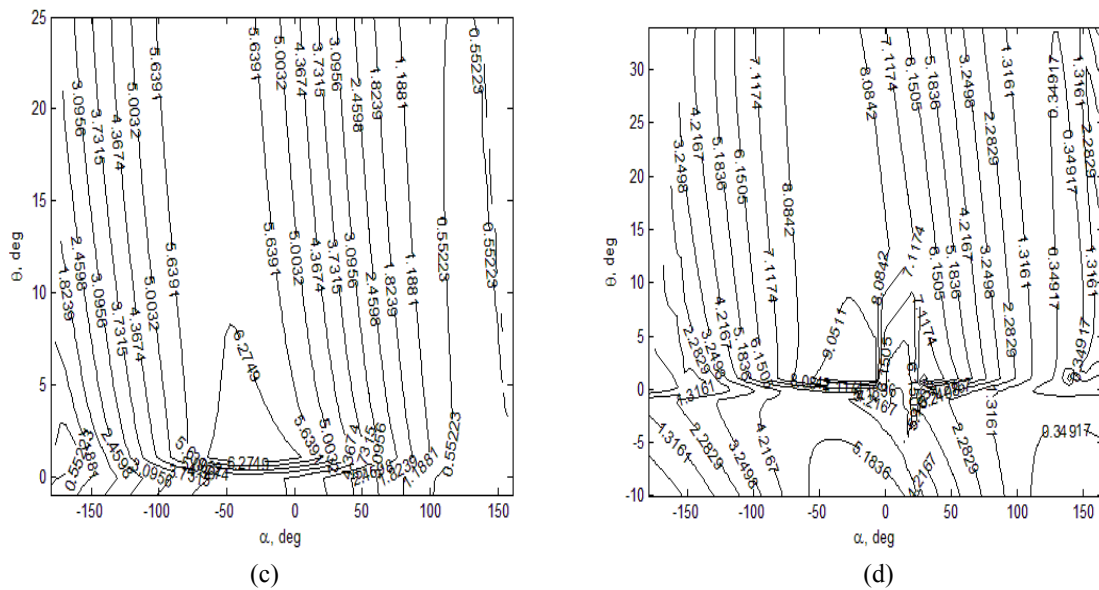


Figure 6 (cont). Variation of energy (in canonical units) as a function α and θ , for $e = 0.2$, $\delta V = 2.0$ C.U., (a) $v = 0^\circ$, (b) $v = 90^\circ$, (c) $v = 180^\circ$ and (d) $v = 270^\circ$.

The next figures makes an overview of the results. They show the maximum variation of energy and their respective values of α and θ , for $\delta V = 1.0$ C.U., $\delta V = 2.0$ C.U., $v = 0^\circ, 90^\circ, 180^\circ$ and 270° for all the eccentricities studied. In all the figures the eccentricities are represented by colors, as follow: $e = 0$ is gray; $e = 0.1$ is black; $e = 0.2$ is blue; $e = 0.3$ is pink; $e = 0.4$ is red; and $e = 0.5$ is green. The symbol "o" represents the cases with $\delta V = 1.0$ C.U. and "*" the cases with $\delta V = 2.0$ C.U..

For example, in Fig. 7, the case with larger variation of energy is the "*" green, that represents the case where $e = 0.5$, $\delta V = 2.0$ C.U., $v = 0^\circ$. In this figure it is possible to see that ΔE_{max} is approximately 50 canonical units, with θ approximately -35° and α is -180° . This is in agreement with the results expected from the physical analyses of the system. The larger eccentricity, when the secondary body is at the periapsis, gives the largest variation of energy, due to the larger velocity of M_2 around M_1 . The propulsion is retrograde, because it is better to increase the gains of the gravitational part of the maneuver than using the impulse to increase the energy of the spacecraft. The larger the value of the magnitude of the impulse, the more efficient is the maneuver. Note that, when $\delta V = 4.0$ C.U., the values of the direction of the impulse tends to zero, because the impulse increases in importance when compared to the gravitational part of the maneuver.

To understand the figure it is necessary to observe it in parts. The horizontal axis represents the maximum energy variation. The lower rectangle in the figure has θ in the vertical axis, and the upper rectangle has α in the vertical axis, both for the maximum energy variation. It is possible to observe values of α and θ which resulted in the largest value for the energy variation for each eccentricity and different magnitudes of the impulse.

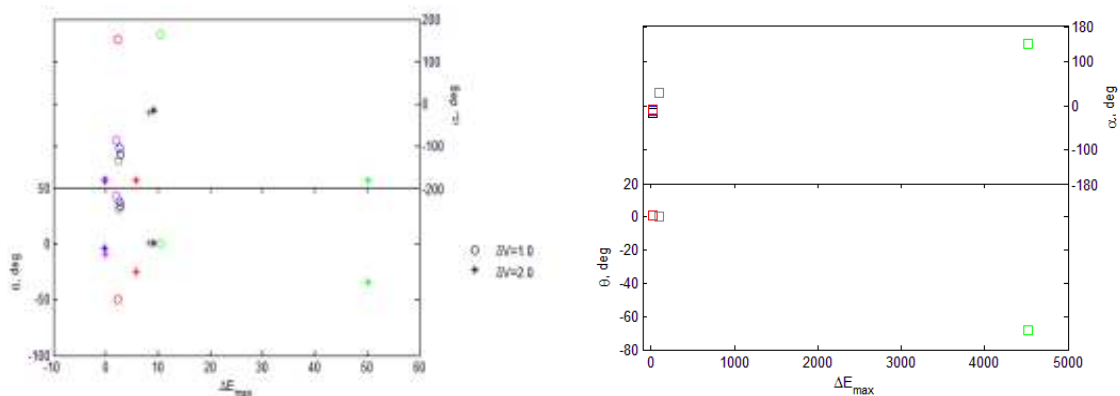


Figure 7. Graph of α vs. ΔE_{\max} and θ vs. ΔE_{\max} , for $v = 0^\circ$, $\delta V = 1.0$ C.U. and $\delta V = 2.0$ C.U. (left), $\delta V = 4.0$ C.U. (right) and the eccentricity given by colors: gray - $e = 0$; black - $e = 0.1$; blue - $e = 0.2$; pink - $e = 0.3$; red - $e = 0.4$; and green - $e = 0.5$.

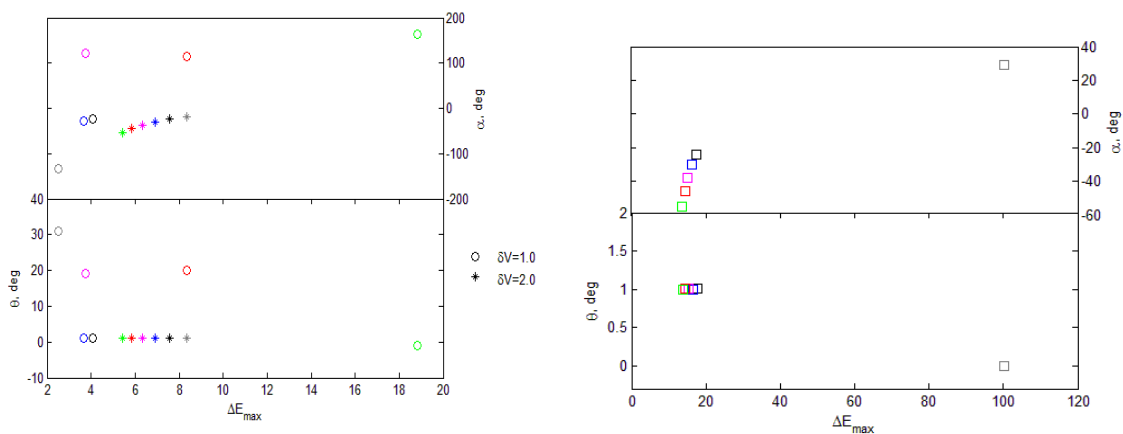


Figure 8. Graph of α vs. ΔE_{\max} and θ vs. ΔE_{\max} , for $v = 180^\circ$, $\delta V = 1.0$ C.U., $\delta V = 2.0$ C.U. (left), $\delta V = 4.0$ C.U. (right) and the eccentricity given by colors: gray - $e = 0$; black - $e = 0.1$; blue - $e = 0.2$; pink - $e = 0.3$; red - $e = 0.4$; and green - $e = 0.5$.

In the configuration shown in Fig. 8, in the moment of the close encounter of the spacecraft with M_2 , M_2 is at the apoapsis of the orbit around M_1 . From this figure we observe that, in several cases, the directions of the impulse are near the direction of motion of the spacecraft, because it is no more interesting to spend the fuel to change the geometry of the system to increase the gains from the gravitational part of the maneuver, since it is weaker now. This fact occurs because the eccentricity decreases the velocity of M_2 with respect to M_1 .

After that, it was also studied maneuvers in the system of Haumea and its moons. Haumea is a dwarf planet, localized in the Kuiper Belt, at a distance of 45 astronomical units from the Sun. Haumea has two natural satellites, Hi'iaka and Namaka. Hi'iaka is the larger one, discovered in January 2005, and the eccentricity of its orbit is 0.0513, and its mass is estimated to be 1.79×10^{19} kg. Namaka was discovered in June 2005, it is the inner moon of Haumea. Its eccentricity is 0.249 and its estimated mass is 1.79×10^{18} kg. The interesting point in studying this system, in particular Haumea-Namaka is due to the large eccentricity of this system. It is excellent to study under the elliptic restricted problem. The next figures show the variation of the energy for different values of true anomaly and the impulse for Haumea-Namaka system. From there, it is possible to obtain the maximum variations of energy in each situation.

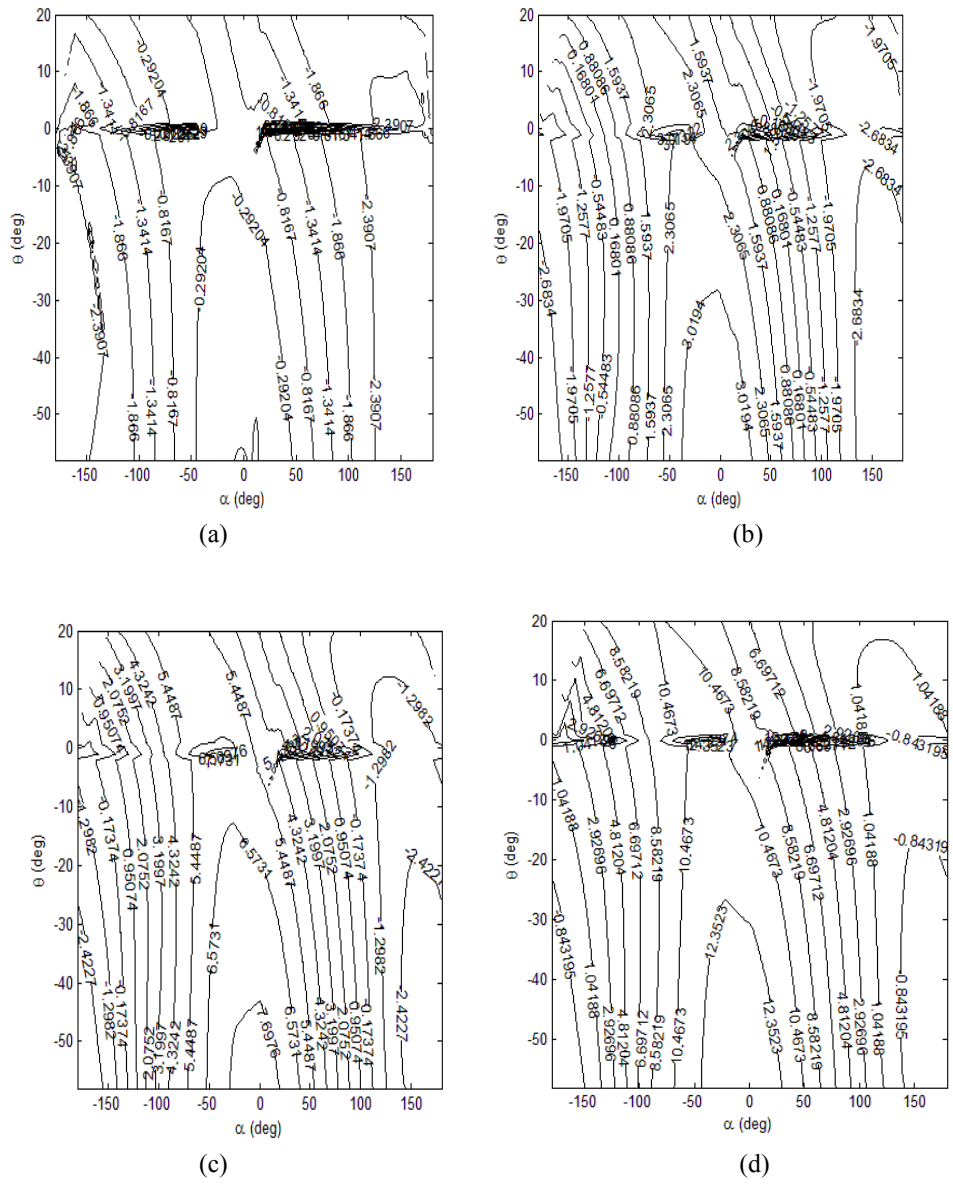


Figure 10. Variation of energy (in canonical units) as a function α and θ , for the Haumea-Namaka system, for $\psi = 270^\circ$, (a) $\delta V = 1.0$ C.U., (b) $\delta V = 2.0$ C.U., (c) $\delta V = 3.0$ C.U., (d) $\delta V = 4.0$ C.U. and $v = 90^\circ$.

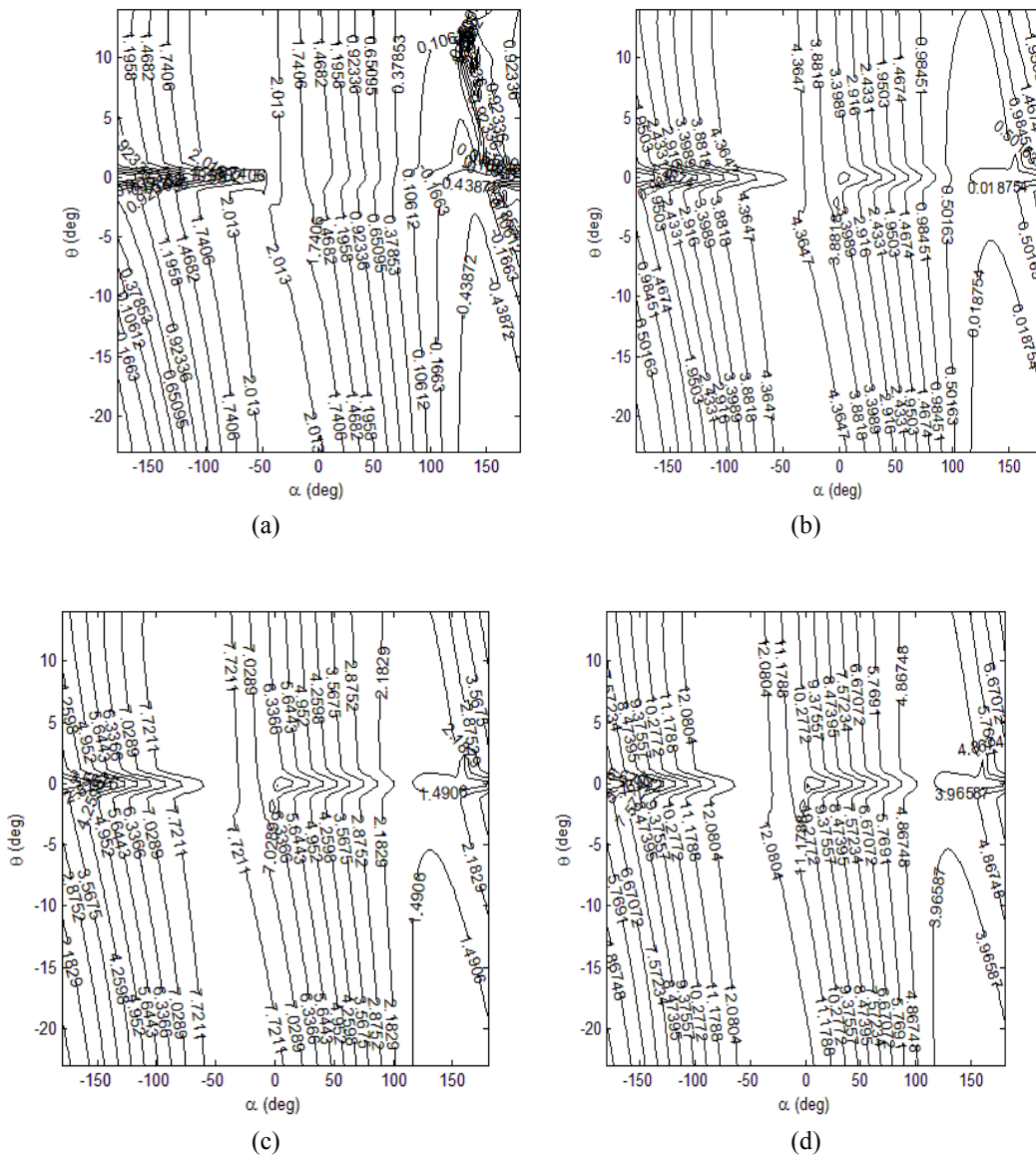


Figure 11. Variation of energy (in canonical units) as a function α and θ , for the Haumea-Namaka system, for $\psi = 270^\circ$, (a) $\delta V = 1.0$ C.U, (b) $\delta V = 2.0$ C.U, (c) $\delta V = 3.0$ C.U, (d) $\delta V = 4.0$ C.U and $\nu = 180^\circ$.

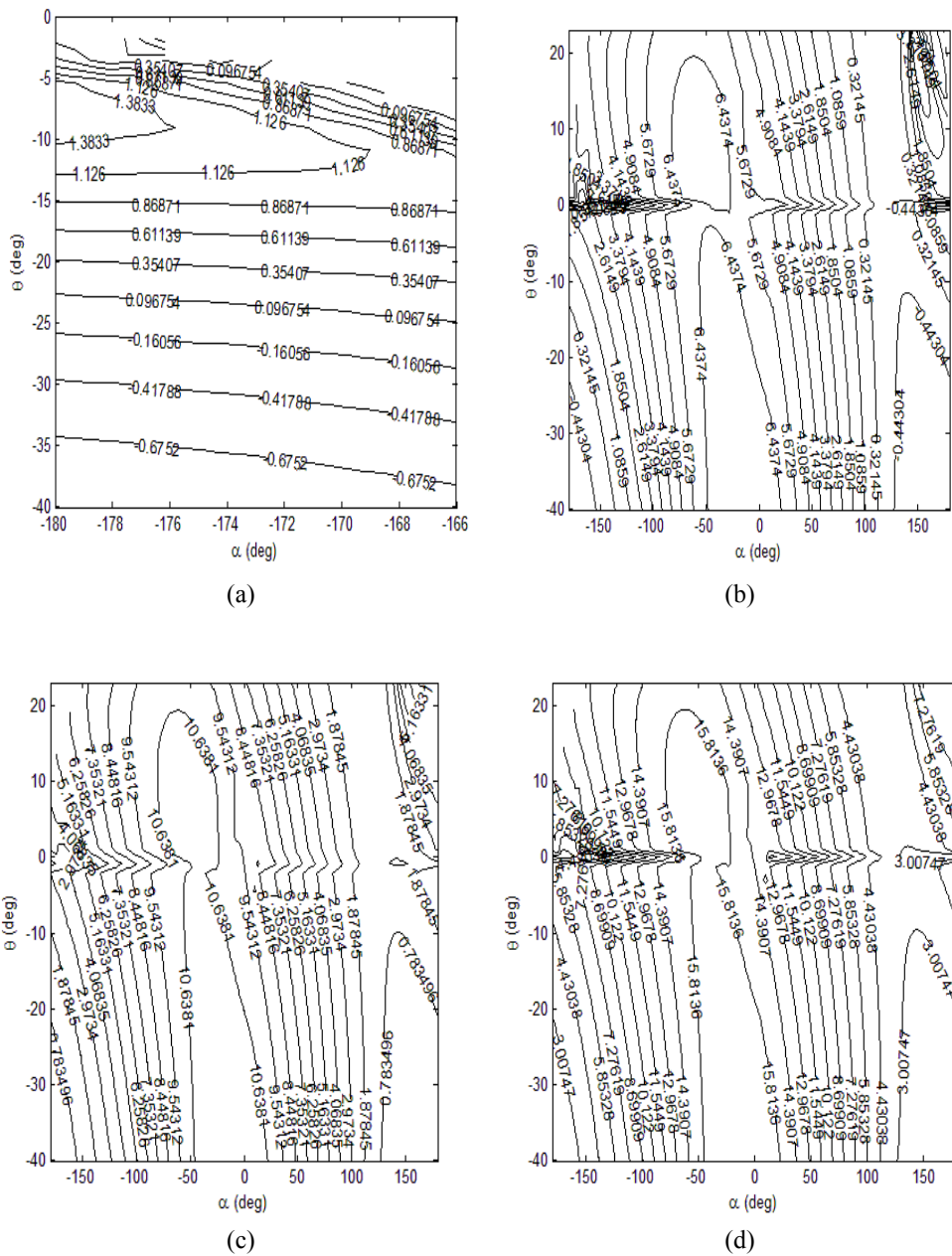


Figure 12. Variation of energy (in canonical units) as a function α and θ , for the Haumea-Namaka system, for $\psi = 270^\circ$, (a) $\delta V = 1.0$ C.U., (b) $\delta V = 2.0$ C.U., (c) $\delta V = 3.0$ C.U., (d) $\delta V = 4.0$ C.U. and $v = 270^\circ$.

The next figure show the trajectories of the spacecraft for the cases that resulted in maximum energy variations for $v = 180^\circ$. The black line is the curve before the impulse and the blue line is the trajectory after the impulse. The black dot represents Haumea. It is shown that the increase of the magnitude of the impulse increases the curvature of the trajectory, so giving more gains in the energy variations due to the gravity part of the maneuver.

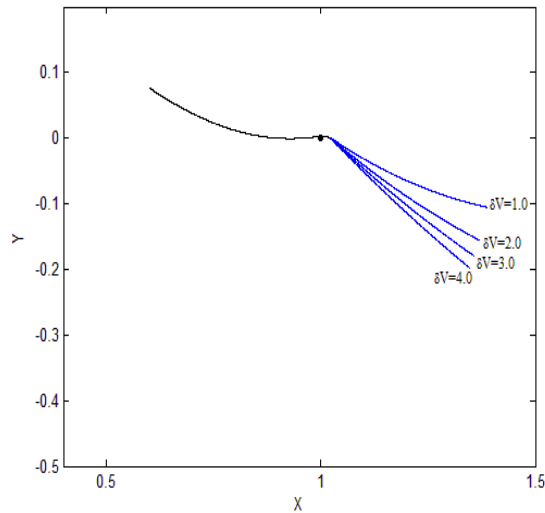


Figure 13. Trajectories of the spacecraft in the Haumea-Namaka system, for $\psi = 270^\circ$, $\delta V = 1.0$ C.U., $\delta V = 2.0$ C.U., $\delta V = 3.0$ C.U., $\delta V = 4.0$ C.U and $\nu = 180^\circ$.

The results confirm and quantify some expected results. For a fixed value of the true anomaly of the body M_2 the energy variations increase with the magnitude of the impulse, in all cases. As an example, for $\nu = 0^\circ$, the values of the variations of energy are: 1.812736, 6.5542055, 12.4799939 and 19.2376467 C.U. for values of the magnitude of the impulse of 1.0, 2.0, 3.0 and 4.0 C.U., respectively. Fixing the magnitude of the impulse, the maximum variations of energy are larger when the body M_2 passes by the periapsis and smaller when it is passing by the apoapsis. Again as an example, since the total data can be read for the figures, when the largest value for the variation of energy comes from the situation where the magnitude of the impulse is 4.0 C.U. and $\nu = 0^\circ$. For the same magnitude of the impulse, the smallest variation of energy occurs for $\nu = 180^\circ$, with a numerical value of 12.9868443 C.U. The directions of the impulses is never in the direction of the motion of the spacecraft, and it alternates from prograde (using the impulse to give energy for the spacecraft) and retrograde directions (searching for increases in the gains from the gravity part of the maneuver). The details can be seen direct from the results shown.

V. Conclusion

The propelled Swing-By maneuver is studied in the situation where M_2 is in an elliptical orbit around M_1 . Since the goal of the maneuver is to gain energy, only situations where the angle of approach is 270° is considered, because this is the region that provides the maximum energy gain. In this way, the maneuver depends on the eccentricity of the primaries, as well as on the true anomaly of M_2 at the moment of the closest approach. In general, the physical effects of including the eccentricity of the primaries is that the velocity of M_2 is no longer constant. The variations of energy is directly proportional to this velocity so, when comparing the Swing-By in the circular problem with the elliptic version, the variation of energy will increase when performed with the secondary body at the periapsis and decrease when performed when the secondary body is at the apoapsis. When considering the propelled Swing-By, the consequence of those facts is that, for some combinations of the eccentricity and magnitude of the impulse and when the passage occurs with M_2 at the periapsis, an impulse in the retrograde direction is more efficient, because it generates a Swing-By with larger gains, which compensates the losses due to the retrograde impulse. These effects increase with the eccentricity. So, when compared with the circular case, the impulses changed from prograde to retrograde, to use the larger effects offered by the close approach in the elliptic case. In the opposite direction, when M_2 is at the apoapsis, the opposite occurs, and the energy variations are smaller when compared to the circular case, so the impulses are always prograde. In general, even with the effect of the eccentricity and the true anomaly of M_2 , it was found that the best conditions for optimal energy variation is when the impulse is not applied in the tangential direction ($\alpha \neq 0^\circ$). The optimal solutions are shown in several circumstances

Acknowledgments

The authors wish to express their appreciation for the support provided by grants # 473387/2012-3 and 304700/2009-6, from the National Council for Scientific and Technological Development (CNPq); grants # 2011/09310-7, 2012/21023-6 and 2011/08171-3, from São Paulo Research Foundation (FAPESP) and the financial support from the National Council for the Improvement of Higher Education (CAPES).

References

- ¹Prado, A.F.B.A., "Powered Swing-By," *Journal of Guidance, Control and Dynamics*, Vol. 19, No. 5, 1996, pp. 1142, 1147.
- ²Prado, A.F.B.A., "Close-Approach Trajectories in the Elliptic Restricted Problem," *Journal of Guidance, Control and Dynamics*, Vol. 20, No. 4, 1997, pp. 797, 802.
- ³Sukhanov, A.A., Velho, H.F.C., Macau, E.E., Winter, O.C., "The Aster Project: Flight to a Near-Earth Asteroid," *Cosmic Research*, Vol. 48, No. 5, 2010, pp. 443, 450.
- ⁴Araújo, R.A.N., Winter, O.C., Prado, A.F.B.A., Sukhanov, A.A., "Stability Regions Around the Components of the Triple System 2001SN₂₆₃," *Monthly Notices of the Royal Astronomical Society*, Vol. 423, 2012, pp. 3058, 3073.
- ⁵Broucke, R. A., "Stability of Periodic Orbits in the Elliptic, Restricted Three-Body Problem," *AIAA Journal*, Vol. 7, No. 6, 1969, pp. 1003, 1009.
- ⁶Broucke, R. A., "The Celestial Mechanics of Gravity Assist," AIAA Paper 88-4220, Aug. 1988.
- ⁷Longuski J.M., Williams S.N., "The Last Grand Tour Opportunity to Pluto," *Journal Astronautic Science*, Vol. 39, 1991, pp. 359, 365.
- ⁸Weinstein, S.S., "Pluto Flyby Mission Design Concepts for Very Small and Moderate Spacecraft," AIAA paper 92-4372, Aug. 1992.
- ⁹Mcconaghy, T. T., Debban, T. J., Petropulos, A. E., Longuski, J. M., "Design and Optimization of Low-Thrust Gravity Trajectories with Gravity Assist," *Journal of Spacecraft and Rockets*, Vol. 40, No. 3, 2003, pp. 380, 387.
- ¹⁰Okutsu, M., Yam, C.H., Longuski, J.M., "Low-thrust Trajectories to Jupiter via Gravity Assists from Venus, Earth and Mars," AIAA Paper 2006-6745, 2006.
- ¹¹Vieira Neto, E., Winter, O.C., "Time Analysis for Temporary Gravitational Capture: Satellites of Uranus," *Astronomical Journal*, Vol. 122, 2001, pp. 440.
- ¹²Szebehely, V., *Theory of Orbits*, Academic, New York, 1967, Chap. 10.